

# Diffuser Effect On The Buoyancy-driven Airflow inside a Solar Chimney Power Plant

Hichem Boulechfar<sup>#1</sup>

<sup>#1</sup>*Faculty of Sciences, Department of physics, University of M'sila, Med Boudiaf University of M'sila, Bordj Bou Arreridj road, M'Sila 28000 Algeria*

<sup>1</sup>[hichem.boulechfar@univ-msila.dz](mailto:hichem.boulechfar@univ-msila.dz)

**Abstract**— The present work analyses numerically the diffuser effect on the buoyancy-driven convection within a solar chimney power plant. The governing equations in our case are continuity, momentum and energy equations in the cylindrical coordinates taking into consideration the Boussinesq approximation. The numerical computation was performed by using Comsol Multiphysics software, based on the finite elements method to solve the system of dimensionless equations considering the simplifying assumptions. The results yielded interesting results regarding the airflow field structure and velocity within the solar chimney, which depend on the geometry of the diffuser that divides the flow and creates optimal locations for dual power-generating turbines.

**Keywords**— Solar chimney, Buoyancy-driven convection, Numerical computation, Diffuser system

## I. INTRODUCTION

The solar conversion systems and their applications represent a broad field of research and development. One such system is solar chimney technology, which has already been implemented and has shown success in various fields. Applications of the solar chimney are diverse, including solar drying processes and water desalination [1]. The solar chimney also plays an important role in natural ventilation when integrated into buildings [2], as well as in electrical power production, which is the main objective of the system. One of the earliest prototypes was designed, constructed, and operated by Schlaich Bergermann [3].

Solar chimney technology and its various applications have been the subject of numerous studies since the first experimental plant in Manzanares. A. Dhahri et al. [4] presented a numerical analysis of the performance of a solar chimney power plant using the steady-state Navier–Stokes and energy equations in a cylindrical coordinate system. The fluid flow inside the chimney was assumed to be turbulent and was simulated using the  $k-\epsilon$  turbulence model in FLUENT.

Shinsuke Okada et al. [5] Siyang Hu et al. [6], and Pranav S. et al. [7] investigated improvements in power generation efficiency through the use of a diffuser-type tower. Both experimental and CFD analyses showed that the diffuser-type tower induced a significant increase in air velocity within the solar chimney.

Tukkee A. M. et al. [8] Studied the entire Solar Vortex Engine (SVE) system to determine the appropriate location of the turbine unit and to demonstrate the capability of the vortex generator to replace the chimney. Three different SVE configurations were compared with corresponding configurations of the Solar Chimney Power Plant (SCPP).

Ghernaout B. et al. [9] and Aseel K. et al. [10] presented experimental and numerical studies on various geometrical and parametric characteristics of solar chimney components, such as collector radius and height. The numerical simulations were performed using a CFD code based on the finite-volume method. Both studies showed good agreement between the experimental and numerical data.

The main objective of the present work is to numerically analyse the effect of a diffuser on the buoyancy-driven flow inside the chimney. The findings will play a crucial role in the design of solar chimneys; furthermore, analysing the diffuser's effect on the flow structure can help determine the number of turbines and their optimal placement, with the aim of improving the efficiency of Solar Chimney Power Plants (SCPPs).

## II. PROBLEM DESCRIPTION

The physical problem presented in this work is governed by a system of partial differential equations (PDEs) that describe natural convection inside a solar chimney, formulated in cylindrical coordinates. The airflow within the solar chimney is generated by buoyancy-driven natural convection, and the model incorporates appropriate assumptions and mathematical formulations using the Boussinesq approximation. The exterior

walls are treated as isothermal and maintained at a constant ambient temperature  $T_c$ , while the ground and the diffuser surfaces that represent the inner walls are considered isothermal at a higher temperature as  $T_h > T_c$ .

A two-dimensional air-updraft solar chimney with axisymmetric geometry, shown in Fig. 1, is described using the dimensionless continuity, momentum, and energy equations. The airflow is assumed to be laminar, steady, and incompressible. Heat conduction and radiation through the collector and chimney walls are neglected, as are viscous dissipation and pressure work in the energy equation.

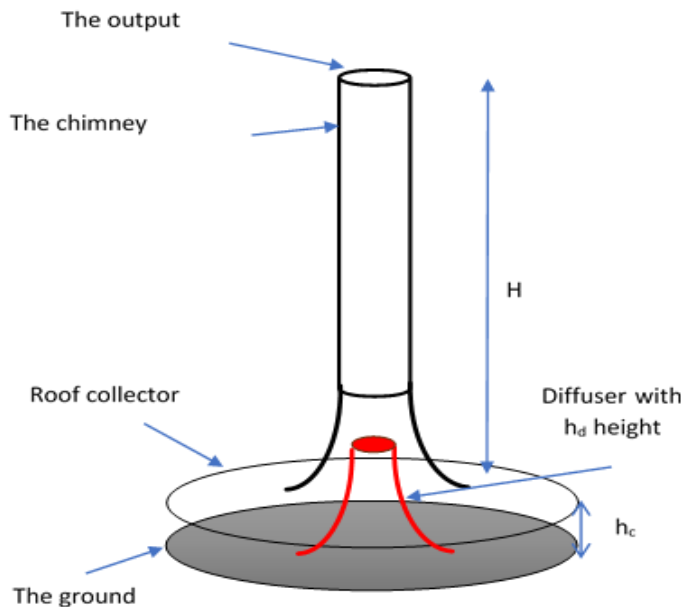


Fig. 1 Solar chimney Geometry

### III. MATHEMATICAL MODEL

#### A. Basic equations in cylindrical coordinates

According to the simplifying assumptions under Boussinesq's approximation, the continuity, momentum, and energy balance equations are formulated as follows:

$$\frac{1}{r} \frac{\partial(rV_r)}{\partial r} + \frac{\partial V_z}{\partial z} = 0 \quad (1)$$

$$\rho \left( V_r \frac{\partial V_r}{\partial z} \right) = - \frac{\partial p}{\partial r} + \mu \left( \frac{1}{r} \frac{\partial}{\partial r} \frac{\partial(rV_r)}{\partial r} - \frac{V_r}{r^2} + \frac{\partial^2 V_r}{\partial z^2} \right) \quad (2)$$

$$\rho \left( V_r \frac{\partial V_z}{\partial r} \right) = - \frac{\partial p}{\partial z} g_z \rho \beta_T (T - T_0) + \mu \left( \frac{1}{r} \frac{\partial}{\partial r} \frac{\partial(rV_z)}{\partial r} + \frac{\partial^2 V_z}{\partial z^2} \right) \quad (3)$$

$$V_r \frac{\partial T}{\partial r} + V_z \frac{\partial T}{\partial z} = \frac{\lambda}{\rho C_p} \left( \frac{1}{r} \frac{\partial}{\partial r} \left( r \frac{\partial T}{\partial r} \right) + \frac{\partial^2 T}{\partial z^2} \right) \quad (4)$$

The Boussinesq's approximation is used for the variations of the density in the buoyancy (body force) term and where the density change is directly correlated with the temperature T. A reference temperature  $T_0$  is used to evaluate the fluid's physical properties, which are assumed constant in all other terms of the above equations, the approximation is expressed in eq. (5):

$$\rho = \rho_0 (1 - \beta_T (T - T_0)) \quad (5)$$

The coefficient of thermal expansion is given by eq. (6):

$$\beta_T = - \frac{\frac{1}{\rho_0} \frac{\partial P}{\partial T}}{\rho_0 \frac{\partial T}{\partial T}} \quad (6)$$

### B. Dimensionless mathematical model

It's suitable to use dimensionless model equations in our case in order to discretize them using a numerical method and to make appearing the controlling parameters such as Rayleigh ( $R_a$ ) and Prandtl numbers ( $P_r$ ) by using dimensionless variables expressed as following:

$$r^+ = \frac{r}{D}, z^+ = \frac{z}{D}, T^+ = \frac{T - T_c}{T_h - T_c}, P^+ = \frac{P}{\rho(\alpha/D)^2}$$

$$V_r^+ = \frac{V_r}{(\alpha/D)}, V_z^+ = \frac{V_z}{(\alpha/D)}$$

1) *Continuity equation:*

$$\frac{1}{r^+} \frac{\partial(r^+ V_r^+)}{\partial r^+} + \frac{\partial V_z^+}{\partial z^+} = 0 \quad (7)$$

2) *Momentum conservation equations:*

$$V_r^+ \frac{\partial V_r^+}{\partial r^+} + V_z^+ \frac{\partial V_r^+}{\partial z^+} = - \frac{\partial p^+}{\partial r^+} + P_r \left( \frac{1}{r^+} \frac{\partial}{\partial r^+} \frac{\partial(r^+ V_r^+)}{\partial r^+} - \frac{V_r^+}{r^{+2}} + \frac{\partial^2 V_r^+}{\partial z^{+2}} \right) \quad (8)$$

$$V_z^+ \frac{\partial V_z^+}{\partial r^+} + V_z^+ \frac{\partial V_z^+}{\partial z^+} = - \frac{\partial p^+}{\partial z^+} + P_r \left( \frac{1}{r^+} \frac{\partial}{\partial r^+} \frac{\partial(r^+ V_z^+)}{\partial r^+} + \frac{\partial^2 V_z^+}{\partial z^{+2}} \right) + R_a \cdot P_r \cdot T^+ \quad (9)$$

3) *Energy equation:*

$$V_r^+ \frac{\partial T^+}{\partial r^+} + V_z^+ \frac{\partial T^+}{\partial z^+} = \frac{1}{r^+} \frac{\partial T^+}{\partial r^+} + \frac{\partial^2 T^+}{\partial r^{+2}} + \frac{\partial^2 T^+}{\partial z^{+2}} \quad (10)$$

### C. Dimensionless boundary conditions:

The boundary conditions in two-dimensional geometry are summarized in Fig. 2.

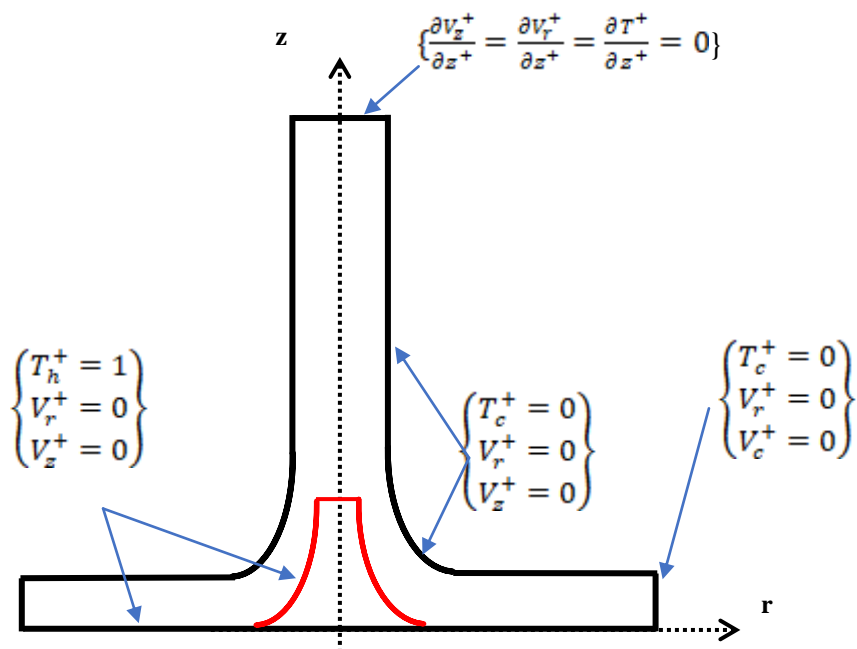


Fig. 2 Dimensionless boundary conditions

#### IV. RESULTS

The results present the findings focusing on the impact of the geometric parameter of the diffuser on the development of airflow within the solar chimney, illustrated through isolines of dimensionless velocity and temperature, along with profiles of the vertical velocity component, which directly correlated with the power production using turbines. Fig.3 to Fig. 6 present velocity and temperature fields for two cases, with and without the diffuser system when Rayleigh number  $Ra=5\times 10^5$ .

##### A. Effect of the diffuser on the temperature and velocity with $Ra=5\times 10^5$

###### 1) Without diffuser ( $h_d/h_c = 0$ )

The observation in Fig. 3(a) represents a fully developed natural convection throughout the solar chimney. This is manifested as a distortion of the isothermal lines, which are lines of constant temperature, across the entire system. This distortion indicates the dominance of the convective mode in the heat transfer when the temperature distribution is decreasing from the hot surface which is a direct result of the increased natural convection. Fig. 3(b) provides a detailed view of this phenomenon; it illustrates a presence of counter-rotating cells at the top of the chimney's entrance. These counter-rotating cells are areas where the air circulates in opposite directions and this circulation is mediated by a primary cell that is moving upwards. The upward movement of this primary cell is critical as it represents the generation of airflow under a convective mode. In the context of a solar chimney, this convective mode is crucial. The heat from the sun warms the air inside the chimney, causing it to rise (due to the buoyancy effect). As the warm air rises, it creates a pressure difference that drives the airflow that will drive a turbine and generate power. Therefore, the observation of an increase in natural convection, as indicated by the distortion of the isothermal lines and the intensification of the counter-rotating cells in Fig. 3, is a positive indication of the system's performance.

###### 2) Diffuser with height ratio ( $h_d/h_c = 0.5$ )

In Fig 4(a), we observe that isotherms are lines that connect points of equal temperature, and they provide a visual representation of the temperature distribution within a system. In this case, the isotherms are showing how heat is distributed within the solar chimney. The deformation of natural convection throughout the entire system is suggested by the warping of these isothermal lines. Moving on to Fig. 4(b), it illustrates an intensified presence of counter-rotating cells at the top of the chimney's entrance due to installation of a diffuser in this area. These counter-rotating cells are more closed but with less velocity due to the area restriction around the diffuser. As we can notice the dimensionless velocity  $U^+$  has decreased from 135 in the case of no diffuser to 106 with a diffuser at a ratio of 0.5. This decrease is mainly due to the space restriction caused by the diffuser, as the natural convection require enough free space for its development, the diffuser in this case will slow down the intensification of the airflow.

###### 3) Diffuser with height ratio ( $h_d/h_c = 1$ )

Fig. 5(a) shows isotherms for  $Ra=5.10^5$  in the case of diffuser height  $h_d/h_c=1$  where we can see a complete distortion of the isothermal lines, which are lines connecting points of equal temperature, is observed. This distortion is a clear demonstration of the dominance of natural convection heat transfer within the system. At the entrance of the chimney, there is a noticeable airflow, indicating that the system is effectively drawing air into the chimney. In Fig. 5(b) which represent the airflow velocity distribution there is no change under the collector area, which is the part of the solar chimney where solar radiation is converted into thermal energy. Contrary, in the junction area of the chimney a noticeable change has occurred in the airflow due to the convective cells fusion from 5 small cells to 3 big cells in the entrance area of the chimney. The increase of the diffuser height has impacted the airflow negatively by reducing its intensity represented by the dimensionless air velocity  $U^+$  from 106 to 87.

###### 4) Diffuser with ( $h_d/h_c = 1.5$ )

In Fig. 6(a) we notice that isothermal lines distribution is similar to the previous figures for different diffuser heights. But when we observe the Fig. 6(b) we notice a significative change qualitatively and quantitatively. The counter-rotating cells split up and became four main cells, two in each side of the chimney with a slight increase in the maximum dimensionless resultant velocity  $U^+$ .

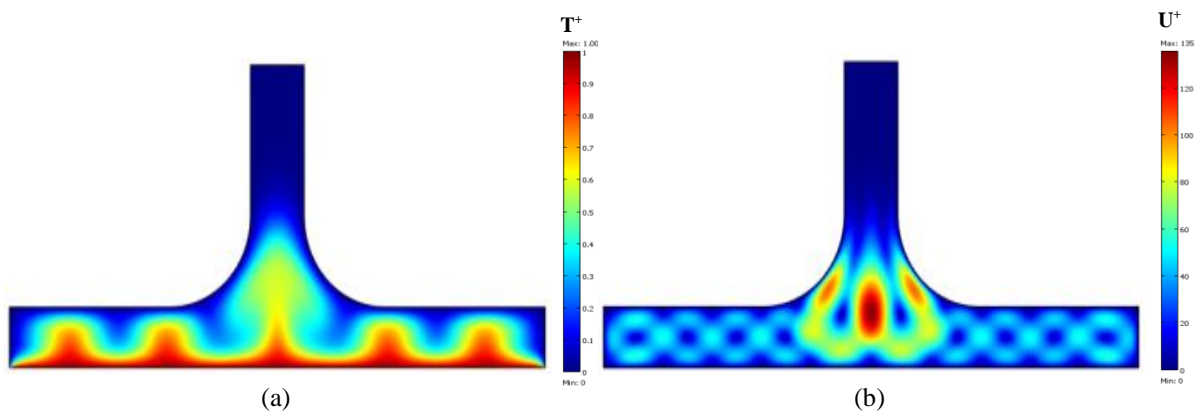


**Fig. 3** (a) Dimensionless temperature distribution, (b) dimensionless velocity field without diffuser ( $h_d/h_c = 0$ ) and  $Ra=5.10^5$

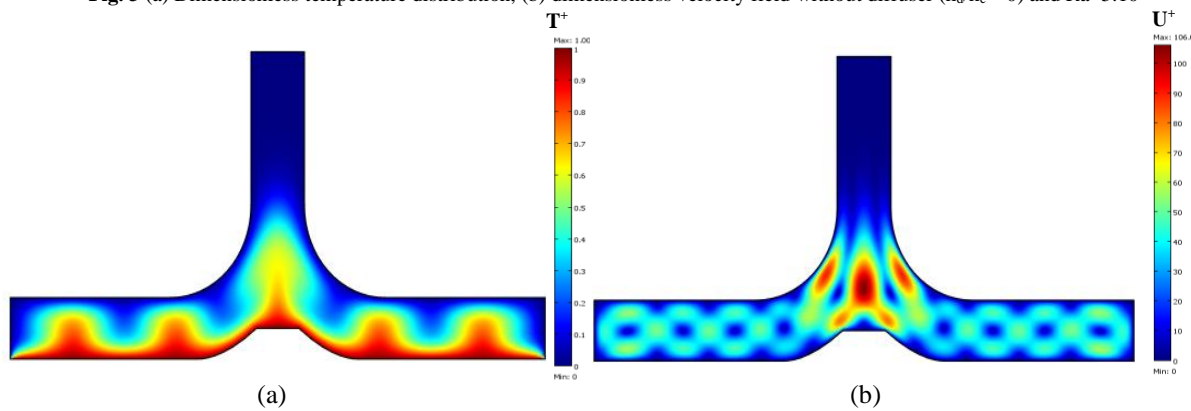


**Fig. 4** (a) Dimensionless temperature distribution, (b) dimensionless velocity field with diffuser height ratio ( $h_d/h_c = 0.5$ ) and  $Ra=5.10^5$

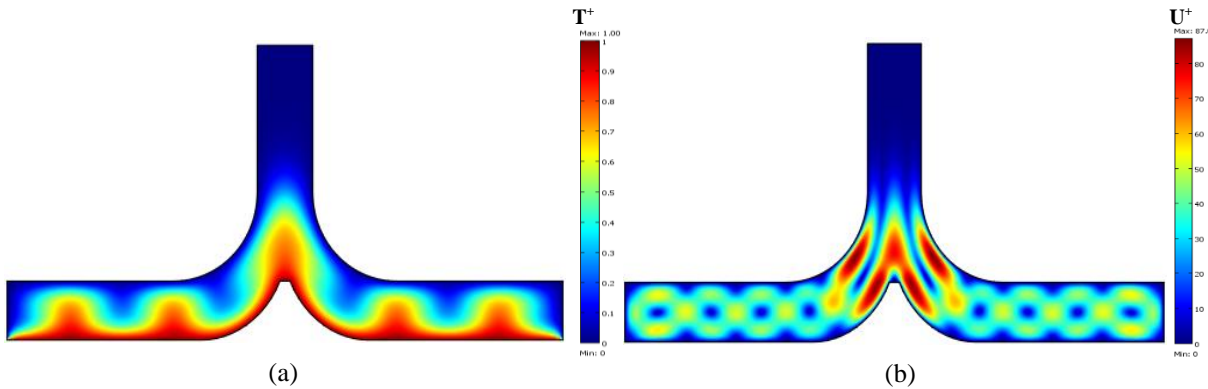


**Fig. 5** (a) Dimensionless temperature distribution, (b) dimensionless velocity field with diffuser height ratio ( $h_d/h_c = 1$ ) and  $Ra=5.10^5$

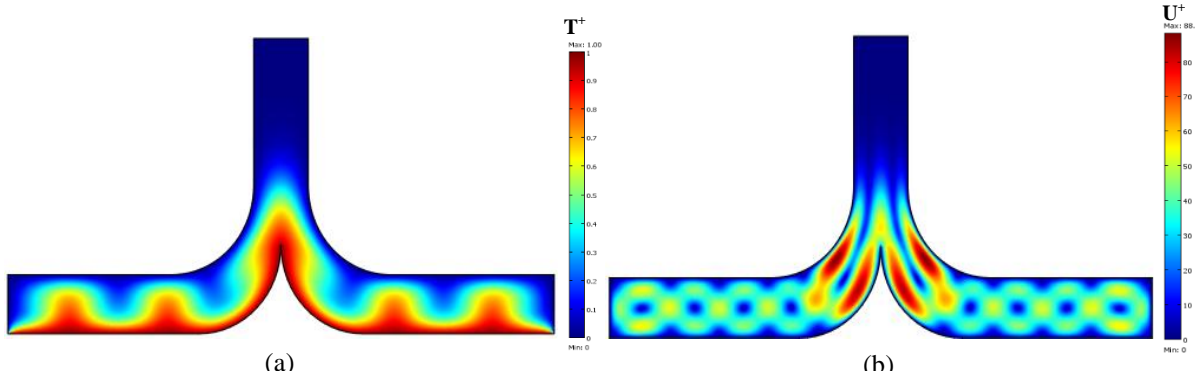


**Fig. 6** (a) Dimensionless temperature distribution, (b) dimensionless velocity field with diffuser height ratio ( $h_d/h_c = 1.5$ ) and  $Ra=5.10^5$

### B. Effect of the diffuser height on airflow dimensionless vertical velocity

Examining Fig. 7(b), which showcases the axial variation of dimensionless vertical airflow velocity across various diffuser heights while maintaining a fixed Rayleigh value of  $Ra=5.10^5$ , we discern a notable trend. Elevating the diffuser height slow down the development of airflow throughout the space, this is resulting in a progressive decrease in velocity magnitude. Illustratively, considering the case without diffuser, the dimensionless vertical velocity peak registers at 140, compared to a peak around 55 observed for a height ratio of 1.5. This height differential yields a substantial enhancement the smoothness flow path but in the same time to reduce the amplitude of the airflow velocity. In addition, Fig. 7(b) shoe that the use of a diffuser divides the flow in two main regions of high velocities instead of only one in the case of a chimney without diffuser.

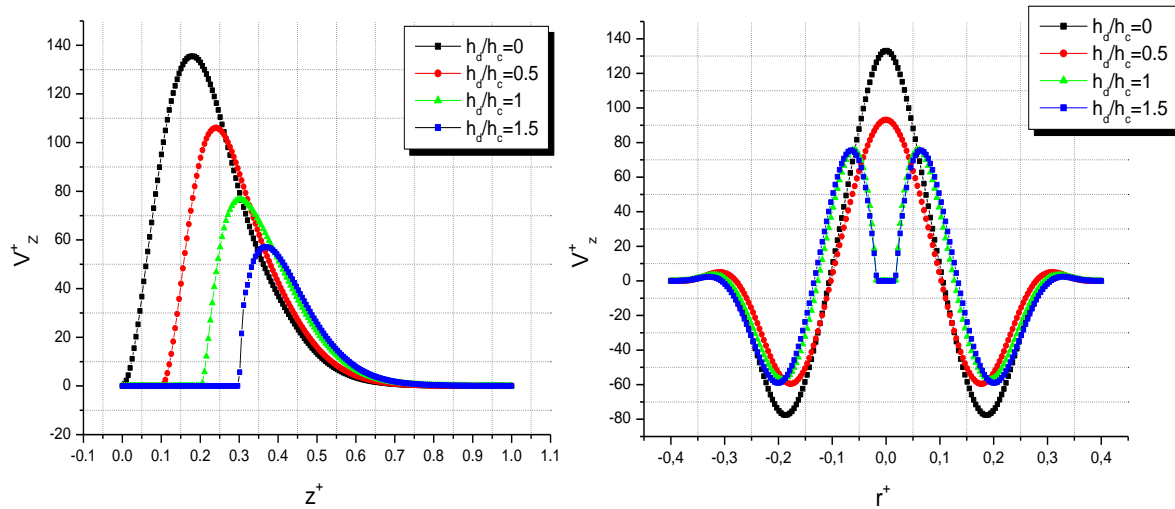


Fig. 7 (a) Axial variation of  $(V_z^+)$ , (b) Radial variation of  $(V_z^+)$  for different height ratio  $(h_d/h_c)$  with  $Ra=5.10^5$

### V. CONCLUSIONS

In our parametric study, we performed a numerical simulation of an axisymmetric solar chimney using COMSOL Multiphysics software. The objective was to simulate the airflow velocity and flow structure generated by natural convection within the solar chimney. To achieve this, we applied the Boussinesq approximation and adopted several assumptions, including laminar flow, steady-state conditions, Newtonian fluid behaviour, and incompressibility. The governing mathematical model was formulated using a system of partial differential equations (PDEs) expressed in cylindrical coordinates.

We investigated the impact of the diffuser height on natural convection inside the solar chimney. Our findings revealed that a solar chimney without a diffuser provides the optimal geometry for achieving the highest efficiency associated with maximum vertical airflow velocity. We concluded that the performance of the solar chimney is closely linked to variations in diffuser height. The results showed that reducing the diffuser height promotes smoother and more intensified airflow development throughout the entire chimney. Moreover, this study enabled us to identify the optimal turbine placement zones to ensure maximum efficiency.

The inclusion of a diffuser in buoyancy-driven airflow conditions constrains the flow and divides it into two main regions for turbine placement, rather than a single optimal location with higher driving air velocity, as observed in the non-diffuser configuration.

## REFERENCES

- [1] Cristiana B. Maiaa et al., "An overview of the use of solar chimneys for desalination," Solar Energy Volume 183, pp. 83-95, 1 May 2019.
- [2] Billal Belfegas et al., "Experimental and Theoretical Investigation on a Solar Chimney System for Ventilation of a Living Room. Mathematical Modelling of Engineering Problems," Vol. 8, No. 2, pp. 259-266, April 2021.
- [3] W. Haaf, K. Friedrich et al., "Solar Chimneys: Part I: Principle and Construction of the Pilot Plant in Manzanares," International Journal of Solar Energy, 2, No. 1, pp.3-20, 1984.
- [4] A. Dhahri et al., "Numerical Study of a Solar Chimney Power Plant," Research Journal of Applied Sciences, Engineering and Technology 8(18): pp.1953-1965, 2014.
- [5] Shinsuke Okada et al., "Improvement in Solar Chimney Power Generation by Using a Diffuser Tower," J. Sol. Energy Eng., 137(3), 031009, 2015.
- [6] Siyang Hu et al., "Numerical modelling and comparison of the performance of diffuser type solar chimneys for power generation," Applied Energy, Volume 204, pp. 948-957, 2017.
- [7] Pranav S. Sawant, Aniket A. Gor, "Effect of a diffuser tower on the power output of a solar chimney power plant," International Journal of Research in Engineering and Technology, Volume: 05, Issue: 02, 2016.
- [8] Tukkee A.M. et al., "Assessment of the Turbine Location for Optimum Performance of the Solar Vortex Engine as a Replacement to the Tall Chimney Solar Updraft Power Plant Design," J. Appl. Comput. Mech., 10(1), pp. 38–54, 2024.
- [9] Ghernaout B. et al., "Parametric study of the airflow structure in a solar chimney," International Journal of Heat and Technology, Vol. 38, No. 2, pp. 285-292, 2020.
- [10] Aseel K. et al., "Experimental and Numerical Study of Collector Geometry Effect on Solar Chimney Performance," Al-Khwarizmi Engineering Journal, 12(4), pp. 59-71, 2017.